

## Electronic supplementary Information

### **A Zn<sub>2</sub>GeO<sub>4</sub>-ethylenediamine hybrid nanoribbon membrane as a recyclable adsorbent for the high-efficient removal of heavy metals from contaminated water**

**Li Yu<sup>+</sup>, Rujia Zou<sup>+</sup>, Zhenyu Zhang, Guosheng Song, Zhigang Chen, Jianmao Yang, and Junqing Hu<sup>\*</sup>**

State Key Laboratory for Modification of Chemical Fibers and Polymer Materials, College of Materials Science and Engineering, Research Center for Analysis and Measurement, Donghua University, Shanghai 201620, China

<sup>+</sup>These authors contributed equally to this work

RECEIVED DATE 11<sup>th</sup> July 2011 , hu.junqing@dhu.edu.cn

#### **1. Experimental details**

**1.1 Preparation of the ZGO-EDA hybrid nanoribbons:** Zn<sub>2</sub>GeO<sub>4</sub>-ethylenediamine (ZGO-EDA) hybrid nanoribbons were synthesized by a facile solvothermal route. All chemicals were purchased from Sinopharm Chemical Reagent Co. Ltd. (Shanghai, China) and were used without further purification. In a typical synthesis, 0.52 g of GeO<sub>2</sub> (5 mmol) and 1.10 g of Zn(CH<sub>3</sub>COO)<sub>2</sub>•2H<sub>2</sub>O (5 mmol) were added to a mixed solvent including 35 mL ethylenediamine (EDA) and 15 mL deionized H<sub>2</sub>O. The mixture was stirred for 30 min and then transferred to a stainless Teflon-lined autoclave with 60 mL of inner volume. The autoclave was kept at 180 °C for 24 h in an electric oven, and cooled naturally to room temperature. The product was washed with deionized water and pure alcohol several times to remove any other possible residues, and then dried at 60 °C overnight. Finally, white ZGO-EDA hybrid nanoribbons were obtained.

**1.2 Preparation of the ZGO-EDA membrane materials:** For typical paper-like membranes, a suspension composing pure alcohol and as-obtained ZGO-EDA hybrid nanoribbons was formed by ultrasonic dispersion, and layer-by-layer cast on a piece of nonwoven (with the standing of nonwoven, the ZGO-EDA hybrid nanoribbon membranes possess improved mechanical properties), which was subsequently placed in an electric oven at 60 °C for vaporizing alcohol, leading to the formation of a self-assembled nonwoven-standing membrane of these

ZGO-EDA hybrid nanoribbons

**1.3 Adsorption experiments:** The stock solutions of heavy metal ions or  $\text{Na}^+$  were prepared by dissolving their corresponding nitrate salts in deionized water. The solutions were further diluted to their required concentrations according to our designed adsorption experiments. All the adsorption experiments were operated at a temperature of 15 °C with pH value of 7. All the chemicals were purchased from Sinopharm Chemical Reagent Co. Ltd. (Shanghai, China) and were used without further purification.

**1.4 Characterizations:** Powder x-ray diffraction (XRD) examinations on the as-synthesized products were conducted on a D/max-2550 PC X-ray diffractometer (Rigaku Co., Japan). The morphologies and structures of the ZGO-EDA hybrid nanoribbons were characterized by using a field-emission scanning electron microscope (SEM, Hitachi, S-4800), and a transmission electron microscope (TEM, JEOL, JEM-2010F). Fourier transform infrared (FTIR) spectroscopy investigations were performed on an IR Rrestige-21 FTIR spectrometer (Shimadzu Co., Japan). The content of the heavy metal ions were measured on an ionic coupled plasma-atomic emission spectroscopy (Leeman Co., America). X-ray photoelectron spectroscopy (XPS) spectra were conducted on an Axis Ultra DLD X-ray photoelectron spectroscopy (Kratos Co., Britain).

## 2. Supplementary Figures

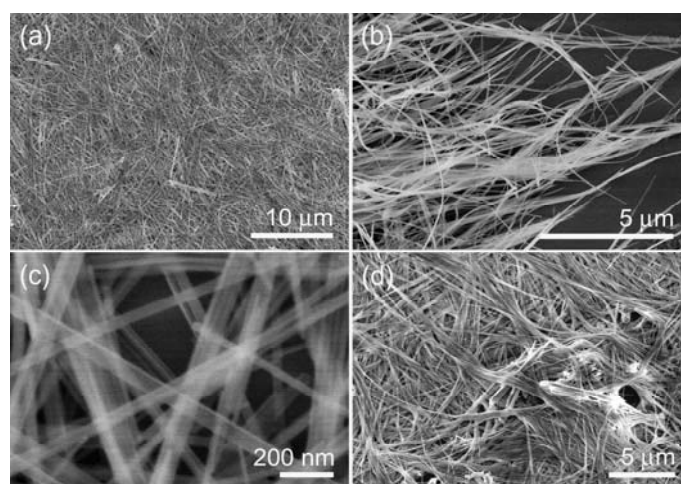


**Fig. S1** (a, b) Low and (c) high-magnification SEM images of the as-synthesized ZGO-EDA hybrid nanoribbons, respectively. (d) Low-magnification SEM image of the ZGO-EDA hybrid nanoribbons annealed at 500 °C for 3 h.

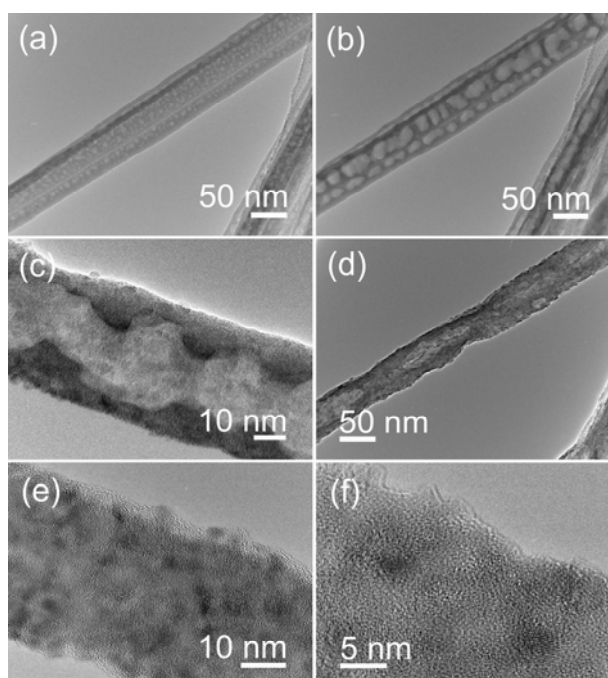


**Fig. S2** TEM images show the structural evolutions of the ZGO-EDA hybrid nanoribbons under in situ electronic beam irradiation within the TEM via a different period: (a) 8 s, (b) 15 s, (c) 60 s, and (d) 100 s. (e) High-magnification and (f) HRTEM images of the irradiated nanoribbon, suggesting that the nanoribbon is consisted of numerous  $\text{Zn}_2\text{GeO}_4$  nanocrystals.

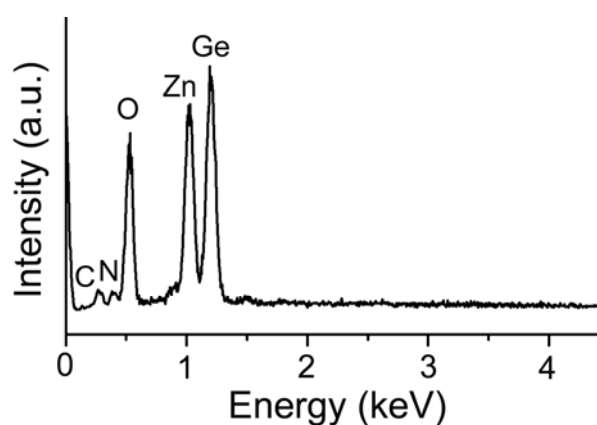


**Fig. S3** Energy dispersive X-ray (EDX) spectrum confirms that the ZGO-EDA hybrid nanoribbons have a chemical composition of C, N, O, Zn and Ge elements.

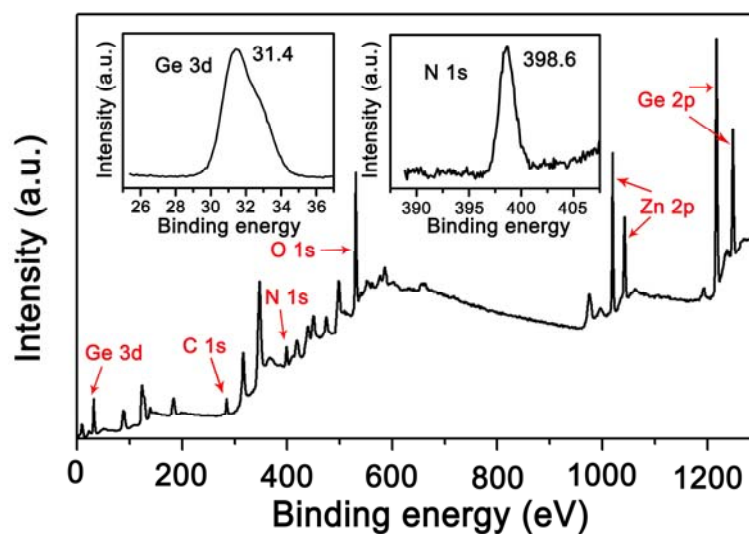


**Fig. S4** The X-ray photoelectron spectroscopy (XPS) of the hybrid nanoribbons. The survey X-ray photoelectron spectroscopy (XPS) reveals that C, N, O, Ge and Zn are present in the  $\text{Zn}_2\text{GeO}_4$ -EDA hybrid nanoribbons. Obviously, the binding energies of Ge 3d, C 1s, N 1s, O 1s, Zn 2p, and Ge 2p of the nanoribbons are 31.4 eV, 286.5 eV, 398.6 eV, 530.2 eV, 1042.5 and 1019.5 eV, 1248.9 and 1217.8 eV, respectively, in which the spectra of the binding energy of Ge 3d and N 1s were detailed in two upper insets of Fig. S4. Among them, the N 1s binding energy of the hybrid nanoribbons is close to that of the N 1s within the alkylamine (399.3 eV or 399.4 eV),<sup>1,2</sup> but not to that of alkylammonium (402.4 eV).<sup>3</sup> So, it can be concluded that the EDA molecules intercalated in the nanoribbons is in the form of  $-\text{NH}_2$  groups, rather than  $-\text{NH}_3^+$  groups.

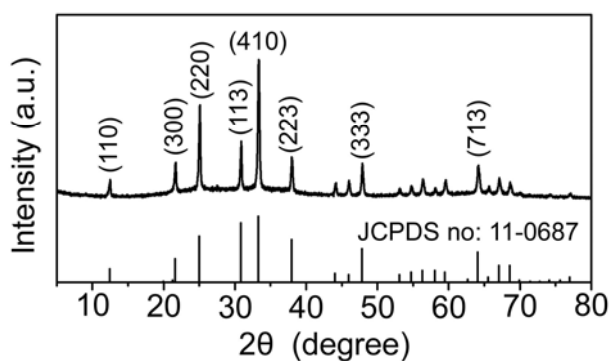


**Fig. S5** XRD patterns of the ZGO-EDA hybrid nanoribbons annealed at 500 °C for 3 h (upper curve) and a standard ZGO powder (bottom curve) from the JCPDS card (11-0687). It can be seen that after being annealed the EDA was lost from this hybrid material, resulting in the formation of rhombohedral phase of Zn<sub>2</sub>GeO<sub>4</sub>.

**Table 1** The adsorption capacity to each ion in different solutions

Sample	Na <sup>+</sup> (mg/g)	Pb <sup>2+</sup> (mg/g)	Cu <sup>2+</sup> (mg/g)	Cd <sup>2+</sup> (mg/g)	Co <sup>2+</sup> (mg/g)
1	0.94	47.97	16.52	4.56	2.75
2	2.43	51.18	16.44	3.77	2.10
3	0.92	104.69	-	-	-
4	0.88	-	55.39	-	-
5	0.56	-	-	40.84	-
6	0.57	-	-	-	16.16

All the concentration of heavy metal ions or Na<sup>+</sup> in the solutions are 5 mM except the sample 2 with Na<sup>+</sup> of 25 mM. From Table 1, we can find that the amounts of adsorption capacity of Na<sup>+</sup> in different solutions are almost less than 1 mg/g, which is much smaller than heavy metal ion species. Comparing the samples 1 and 2, with concentration of Na<sup>+</sup> increasing from 5 mM to 25 mM, the adsorption capacity of the membrane also follows the order of Pb<sup>2+</sup> > Cu<sup>2+</sup> > Cd<sup>2+</sup> > Co<sup>2+</sup>. Additionally, in order to investigate the effect of sodium during adsorption processes, the samples 3, 4, 5 and 6 were designed to give further examinations, which contained each of the different heavy metal ions with Na<sup>+</sup>, respectively. It exhibits that Na<sup>+</sup> does not have obvious influences on adsorption capacity of each heavy metal ion when it is mixed with Na<sup>+</sup> in one solution, i.e., it means whether Na<sup>+</sup> is present or not, it does little concern with the adsorption capacity to all mentioned heavy metal ions.

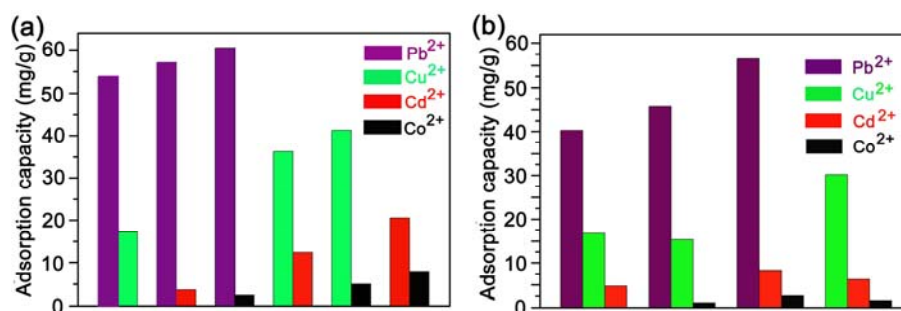


**Fig. S6** The adsorption capacity of heavy metal ions in the binary and ternary systems.

The binary mixture systems contain  $\text{Pb}^{2+}/\text{Cu}^{2+}$ ,  $\text{Pb}^{2+}/\text{Cd}^{2+}$ ,  $\text{Pb}^{2+}/\text{Co}^{2+}$ ,  $\text{Cu}^{2+}/\text{Cd}^{2+}$ ,  $\text{Cu}^{2+}/\text{Co}^{2+}$  and  $\text{Cd}^{2+}/\text{Co}^{2+}$ , Fig. S6a, in which all the concentrations of heavy metal ions in solutions are 5 mM.  $\text{Pb}^{2+}$  in solutions is found to be effectively and favorably adsorbed on the membrane, compared with the other heavy metal ions. However, the existence of competitor species, such as  $\text{Cu}^{2+}$ ,  $\text{Cd}^{2+}$  and  $\text{Co}^{2+}$ , resulting in a great decrease of the amount of  $\text{Pb}^{2+}$ , contrasted with single  $\text{Pb}^{2+}$  in a solution (72.54 mg/g, Fig. 3c, manuscript).

Similarly, in ternary mixtures such as  $\text{Pb}^{2+}/\text{Cu}^{2+}/\text{Cd}^{2+}$ ,  $\text{Pb}^{2+}/\text{Cu}^{2+}/\text{Co}^{2+}$ ,  $\text{Pb}^{2+}/\text{Cd}^{2+}/\text{Co}^{2+}$ ,  $\text{Cu}^{2+}/\text{Cd}^{2+}/\text{Co}^{2+}$  systems, the analogous phenomena to the above are further demonstrated by comparable experiments showed in Fig. S6b, the adsorption capacity equally obeys the order:  $\text{Pb}^{2+} > \text{Cu}^{2+} > \text{Cd}^{2+} > \text{Co}^{2+}$ . Since  $\text{Pb}^{2+}$  shows some advantages of electronegativity, electrode potential and ionic size to that of  $\text{Cu}^{2+}$  and  $\text{Cd}^{2+}$  (even if it should consider a higher atomic weight of  $\text{Pb}^{2+}$ ),  $\text{Pb}^{2+}$  in the solutions are found to be effectively and favorably adsorbed on the membrane, compared with the other metal ions.<sup>4-6</sup> Also, there are several factors can affect the selective adsorption order for different heavy metal ions, such as ionic charge, PH value, and the strong or weak bonds with the diamine ligands, etc.

## References:

- (1) Q. S. Gao, P. Chen, Y. H. Zhang, Y. Tang, *Adv. Mater.*, 2008, **20**, 1837.
- (2) X. L. Hu, Q. M. Ji, J. P. Hill, K. Ariga, *CrystEngComm*, 2011, **13**, 2237.
- (3) R. J. J. Jansen, H. Van Bekum, *Carbon*, 1995, **33**, 1021.
- (4) I. A. Sengil, M. Özacar, *J. Hazard. Mater.*, 2009, **166**, 1488
- (5) S. Y. Zhou, A. L. Xue, Y. J. Zhao, Q. W. Wang, Y. Chen, M. S. Li, W. H. Xing, *Desalination*, 2011, **270**, 269.
- (6) A. J. Du, D. D. Sun, J. O. Leckie, *J. Hazard. Mater.*, 2011, **187**, 96.